Time-dependent analytical *R*-matrix approach for strong-field dynamics. II. Many-electron systems

Lisa Torlina,[1] Misha Ivanov,[1,2,3] Zachary B. Walters,[4,1] and Olga Smirnova[1]

[1]*Max Born Institute, Max Born Strasse 2a, 12489 Berlin, Germany*

[2]*Department of Physics, Humboldt University, Newtonstrasse 15, 12489 Berlin, Germany*

[3]*Department of Physics, Imperial College London, South Kensington Campus, SW7 2AZ London, United Kingdom*

[4]*Max Planck Institute for the Physics of Complex Systems, Nöthnitzer Strasse 38, 01187 Dresden, Germany*

Ionization of atoms and molecules in intense low-frequency fields is a multielectron process which may leave the ion in different excited states. Within the adiabatic perspective on strong-field ionization, usually referred to as optical tunneling, electrons remaining in the molecular ion are assumed to be frozen during the ionization process. In this case, the only way to excite the molecular ion during ionization is to remove an electron from a lower-lying molecular orbital. The higher ionization potential corresponding to such processes implies that such channels are exponentially suppressed during tunneling. Here we show that correlation-induced coupling between the departing electron and the core electrons removes the exponential penalty for ionic excitations, resulting in complex attosecond dynamics of core rearrangement during strong-field ionization. We develop a multichannel theory of strong-field ionization and demonstrate the importance of correlation-induced excitations in the multiphoton and tunneling regimes for N_2 and CO_2 molecules.

I. INTRODUCTION

Ionization is a ubiquitous phenomenon in laser-matter interaction, underlying such diverse processes as the photoelectric effect, radiation damage, tunneling microscopy, and laser-based mass spectroscopy, as well as many others. Even if only one electron escapes the core, ionization at its heart involves interaction between all electrons of the original system. This interaction has been long appreciated in the case of single photon ionization, where different mechanisms such as "shake-up" and postionization interaction ("knock-out" or "two-step-one" process) play a crucial role in describing the rearrangement of the core that may accompany ionization (e.g., see [1–3]).

In most pathways, electron-electron correlation plays a key role. In shake-up, for example, this correlation occurs prior to the absorption of the photon. In simple terms, the "core" electrons feel the presence of the "active" electron before ionization and feel its absence afterwards. The absence is felt in the form of a modified potential, which no longer experiences the contribution of the liberated electron. The old wave function is then projected onto eigenfunctions of the new potential. For shake-up to occur, the active electron must escape more quickly than the core electrons can adjust to its absence, so that the core wave function does not change during the ionization process.

Interaction between the outgoing electron and electrons in the core can also occur after the photon has been absorbed. Part of the departing electron's energy is transmitted to the core, changing the state of the ion in what is essentially a half-collision. Unlike shake-up, this postionization interaction can take time: The long range of the Coulomb interaction allows the escaping electron to interact with the core as it departs.

How will this picture change when not one but many photons are absorbed? For a low-frequency field, the minimum number of photons needed for ionization, $N_0 = I_p/\omega$, may be very large. Here I_p is the ionization potential and ω is the laser frequency. Because multiple photons are absorbed, there are now multiple instances when electron-electron correlation may

be felt. If we were to treat the electron-electron correlation perturbatively, we would have the following intuitive picture: N_1 photons could be absorbed before electron-electron correlation and N_2 photons could be absorbed after for any combination such that $N_1 + N_2 = N_0$. How do such pathways add up? Is it possible for electron-electron interaction to change the state of the core more than once? How important would such higher-order terms in electron-electron correlations be? Here we address these questions.

We apply the time-dependent analytical *R*-matrix (ARM) approach developed in our companion paper [4], generalizing it to N electron systems with one departing electron and $N - 1$ core electrons. Our results generalize the analytical theory of strong-field ionization already developed for single-electron systems [4–7] to the multielectron, multichannel case. In this way, we are able to describe electron rearrangement in the core of an atom or molecule which accompanies strong-field ionization, going beyond the picture of direct ionization developed in [8–11] (see also the so-called SU1 contribution in Ref. [12]). The picture of direct ionization is widely applied in molecules, where it is often viewed (interpreted) as tunneling from a particular molecular orbital. From the perspective of different contributions during tunneling described in Ref. [12], our analysis explicitly incorporates electron-electron interaction throughout the whole motion across the tunneling barrier, not only correlation after the electron emerges from the classically forbidden barrier region (called the SU2 contribution in [12]).

In theories based on the single active electron approximation, excitation of the core during strong-field ionization has long been assumed to be negligible. This is most easily understood in the following simple picture. The binding potential and the time-dependent laser field combine to create an oscillating barrier through which the electron must escape. Aside from the oscillation, this picture is reminiscent of tunnel ionization in static fields. The transmission rate through such a barrier is exponentially suppressed with respect to I_p, not only for static electric fields but also for oscillating laser fields [5]. It has therefore been a nearly universal assumption that the

removal of the least bound electron from the molecule is exponentially dominant, leaving the resulting ion in its lowest electronic state.

The exponential penalty arises in the standard theory of strong-field ionization because the core is either assumed to be frozen during the tunneling process or is described using self-consistent field (see, e.g., [13] for a recent application of this approximation to strong-field ionization). Within the self-consistent field approach, the electron would have to tunnel from a more deeply bound orbital to leave the core in an excited state. Thus, contrary to single-photon ionization, multiphoton ionization in low-frequency fields (optical tunneling) is conventionally treated as an adiabatic process. This perspective is embedded in the theory of inelastic tunneling of [8–11].

Interestingly, this adiabatic picture contradicts the well-known perspective on atom-ion collisions with charge exchange, where the tunneling of an electron from an atom to an ion may involve substantial excitations of the donor [14,15]. Recent experimental advances have also begun to challenge the picture of strong-field ionization as an adiabatic process (see, e.g., [16,17] for the latest evidence of nonadiabatic multielectron dynamics during strong-field ionization).

A nonadiabatic multielectron response implies the presence of excited states of the ion after ionization. In principle, these states could be detected by examining the photoelectron spectra, as done for single-photon ionization. However, the highly nonlinear nature of the strong-field interaction makes such analysis very challenging, obscuring the identification of different ionic states [18]. Alternatively, one could attempt to identify excited states in molecules by the fragmentation channels to which they correlate (see, e.g., Ref. [12]). However, these techniques do not generally allow one to experimentally distinguish ionic excitations that occur during ionization from those that occur after. These problems have now been addressed using coincidence techniques [19], which allow one to correlate energies in the photoelectron spectra with ionic fragments, "cleaning up" the photoelectron spectra and making it possible to distinguish ionic excitations that have occurred during or after ionization. Together with alternative evidence [20–26], experiments have now unambiguously demonstrated a significant contribution of multiple ionization channels, which correspond to a population of different electronically excited states during ionization. Strong experimental arguments suggest that, just like one-photon ionization, multiphoton ionization is not an adiabatic process [16,17,24].

To address these issues, it is necessary to not only consider multiple ionization channels associated with different final states of the ion, but also to include the interaction between these channels during ionization. Loosely speaking, these channels correspond to the removal of electrons from different orbitals. Rigorously, they correspond to different final states of the ion. Interaction between channels is associated with the excitation and deexcitation of the ion, that is, moving the hole from one orbital to another during the ionization process. The importance of channel coupling due to the laser field has been emphasized theoretically in [24,27,28]. The combined effect of the strong laser field and channel coupling on the recombination step of high harmonic generation has been discussed in Ref. [29]. Reference [24] suggested the importance
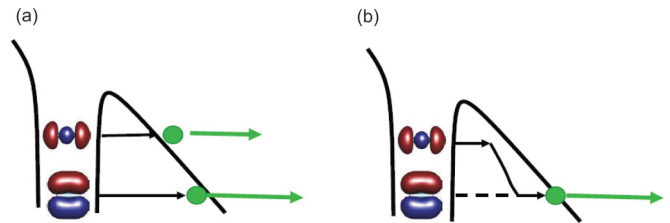
FIG. 1. (Color online) An illustration of the direct (a) and correlation-driven (b) channels in tunnel ionization.

of electron correlations during tunneling and provided the first experimental indication of nontrivial dynamics induced by this coupling. The theory presented below lays the foundation for the analysis and interpretation of these dynamics.

Qualitatively, allowing the state of the ion to evolve during ionization may significantly alter the likelihood of ionizing to an excited final state. Electron-electron correlation between the ion and the departing electron can induce nonadiabatic dynamics as the electron leaves the core. As a result of this excitation, which can happen at any point during ionization (tunneling), the creation of excited ionic states is not subject to the full exponential suppression accompanying direct ionization from more deeply bound orbitals. Figure 1 shows an illustration of this nonadiabatic, correlation-driven pathway. The left panel shows the usual direct adiabatic tunneling channels, corresponding to the removal of an electron from the highest occupied molecular orbital (HOMO) and the one just below it (HOMO-1). A thinner tunneling barrier for the highest orbital gives the first channel an exponential advantage over the second. The right panel shows the nonadiabatic correlation-driven channel. Here the electron leaves from the HOMO. However, before exiting the tunneling barrier, it interacts with the core electrons and excites the ionic core. The tunneling electron then loses its energy and has to pass through a thicker barrier, which corresponds to the HOMO-1 being vacant. However, this thicker barrier appears only at the end, so that the nonadiabatic channel does not incur the full exponential penalty characteristic of the direct HOMO-1 channel.

This paper is organized as follows. Sections II and III present a multichannel theory of strong-field ionization which includes electron-electron correlation during tunneling. In Secs. IV and V we perform saddle-point analysis of the general expressions in the spirit of Perelomov, Popov, and Terent'ev (PPT) theory [6,7] and derive simple analytical expressions for direct and correlation-driven channels in strong-field ionization. Section VI illustrates the importance of correlation-induced excitations for tunnel ionization of N_2 and CO_2 molecules. Section VII discusses the role of this channel in strong-field phenomena.

II. BASIC EQUATIONS

We use the analytical time-dependent R-matrix approach (ARM) [4] and the saddle-point method to develop a multi-channel theory of strong-field ionization. First, we introduce the Hamiltonian of an N-electron neutral molecule interacting

with a laser field:

$$H^N = T_e^N + V_C^N + V_{ee}^N + V_L^N,$$

$$V_C^N = -\sum_{m,i=1}^{i=N} Z_m/|\mathbf{R}_m - \mathbf{r}_i|, \qquad (1)$$

$$V_{ee}^N = \sum_{i\neq j}^N 1/|\mathbf{r}_i - \mathbf{r}_j|, \quad V_L^N = \sum_i \mathbf{F}(t)\cdot\mathbf{r}_i.$$

Here the nuclei with charges Z_m are frozen at positions $\mathbf{R}_m$. Index m enumerates the nuclei, while i, j label the electrons. Superscript N indicates the number of electrons involved. T_e^N is the electron kinetic energy operator, V_C^N describes the Coulomb potential of the nuclei, V_{ee}^N describes the electron-electron interaction, and V_L^N describes the interaction with the laser field.

We also use the Hamiltonian of the ion in the laser field H^{N-1} and the Hamiltonian of an electron H_e interacting with the laser field, the nuclei, and the $(N-1)$ electrons of the ion, $H_e = H^N - H^{N-1}$.

Our goal is to solve the time-dependent Schrödinger equation for the N-electron wave function of the molecule, initially in its ground electronic state $\Psi_g(\mathbf{r})$:

$$i\frac{\partial}{\partial t}|\Psi^N(t)\rangle = \widehat{H}^N|\Psi^N(t)\rangle, \qquad (2)$$

$$|\Psi^N(t=0)\rangle = |\Psi_g\rangle. \qquad (3)$$

Let us now apply the time-dependent ARM approach [4]. We begin by reformulating the initial value problem as a boundary problem. We divide the space into inner and outer regions and introduce the Bloch operator for the outer region $\widehat{L}^-(a)$,

$$\widehat{L}^-(a) = -\sum_{i=1}^N \widehat{\Delta}_i(a)\widehat{B}_i, \qquad (4)$$

where the index i labels each of the N electrons. In coordinate representation we have

$$\langle\mathbf{r}|\widehat{\Delta}_i(a)|\mathbf{r}'\rangle = \delta(r_i - a)\langle\mathbf{r}|\mathbf{r}'\rangle = \delta(r_i - a)\delta(\mathbf{r} - \mathbf{r}'), \quad (5)$$

$$\langle\mathbf{r}|\widehat{B}_i|\mathbf{r}'\rangle = \left(\frac{d}{dr_i} - \frac{b_0 - 1}{r_i}\right)\delta(\mathbf{r} - \mathbf{r}'). \qquad (6)$$

Here b_0 is an arbitrary constant (see, e.g., [4] for discussion). We use the shorthand notation $\widehat{\Delta}(a)\widehat{B} \equiv \sum_i \widehat{\Delta}_i(a)\widehat{B}_i$ to imply summation over all electrons. The δ function is defined such that

$$\int_a^\infty dr\,\delta(r-a) = \int_0^a dr\,\delta(r-a) = \frac{1}{2}. \qquad (7)$$

Adding and subtracting the Bloch operator to the Hamiltonian, we can rewrite Eqs. (2) and (3) as

$$i\frac{\partial}{\partial t}|\Psi^N(t)\rangle = [\widehat{H}^N + \widehat{L}^-(a)]|\Psi^N(t)\rangle - \widehat{L}^-(a)|\Psi^N(t)\rangle,$$

$$|\Psi^N(t=0)\rangle = |\Psi_g^N\rangle. \qquad (8)$$

The boundary nature of the Bloch operator allows one to reformulate Eqs. (8) as a boundary value problem, with the

formal solution

$$|\Psi^N(t)\rangle = -i\int_{-\infty}^t dt'\, U^N(t,t')\widehat{\Delta}(a)\widehat{B}|\Psi^N(t')\rangle. \qquad (9)$$

Here $U^N(t,t')$ is the N-electron propagator in the outer region, corresponding to the outer-region Hamiltonian $\widehat{\mathcal{H}}^N = \widehat{H}^N + \widehat{L}^-(a)$.

We now use the same approach as in the one-electron case [4] and approximate the wave function on the right-hand side of Eq. (9) with the ground state of the neutral atom, $|\Psi^N(t')\rangle \simeq e^{-iE_g t'}a_g(t')|\psi_g^N\rangle$, yielding

$$|\Psi^N(t)\rangle = -i\int_{-\infty}^t dt'\, U^N(t,t')\widehat{\Delta}(a)\widehat{B}|\psi_g^N\rangle a_g(t')e^{-iE_g t'},$$

$$(10)$$

where E_g is the energy of the ground state and $a_g(t')$ incorporates Stark shift and the depletion of the ground state. Our next step is to introduce a multichannel expansion into the above equation.

III. MULTICHANNEL FORMALISM

A. Selection of channels

At this point, we need to identify the ionization channels associated with different states of the ion. The key aspect we have to consider is the presence of the strong laser field, which can induce multiple transitions in the ion and in the continuum.

At first glance, one might like to introduce channels which (i) incorporate the effects of the strong laser field fully and (ii) lead to well-defined field-free states of the ion at the end of interaction $t = T$. Referring to Eq. (10), this implies projecting the final wave function $|\Psi^N(T)\rangle$ on the field-free ionic states $\langle n|$ at $t = T$. According to Eq. (10), these states $\langle n|$ would then have to be propagated back in time from T to t', with potentially complex evolution. Each channel defined in this way may incorporate not only multiple bound but also continuum states of the ion. Such complexity is undesirable.

To avoid backpropagation, one could instead project onto field-free states of the ion at the moment t', as the wave function is transferred through the boundary between the inner and outer regions. However, given our goal of an analytical description, this standard choice is also far from ideal. Indeed, since the ion is created in the presence of a strong laser field, ionic states populated during ionization are likely to be far from their field-free counterparts. Distortion of the field-free ionic states has to be included in the ionization step.

To find a good compromise, we recall the dynamics of single-channel strong-field ionization. First, ionization occurs in bursts centered around the instantaneous maxima of the oscillating laser field. Second, the transition to the continuum during each ionization burst is described by trajectories moving in complex time, with the ionization step essentially completed when the trajectory descends to the real time axis. This time interval constitutes a small fraction of the laser period. Thus, the required ionic basis states should (i) be relatively straightforward to find, (ii) incorporate the strong laser field, and (iii) minimize laser-induced transitions during

the (complex-valued) fraction of the laser cycle associated with the ionization step itself: the electron motion in the classically forbidden region. For these reasons, we associate different channels with quasistatic states of the ion, also known as "field-polarized" and/or "adiabatic."

These states, denoted as $|\mathfrak{n}_t\rangle$, satisfy the stationary Schrödinger equation for the time-dependent ionic Hamiltonian H^{N-1} which includes the laser field. They are defined by the equation

$$H^{N-1}|\mathfrak{n}_t\rangle = E_n^{N-1}(t)|\mathfrak{n}_t\rangle \qquad (11)$$

and follow the laser field adiabatically. They are found by diagonalizing the Hamiltonian of the ion in the laser field H^{N-1} at each moment of time. In practice, such diagonalization requires knowledge of the ionic field-free states, including their energies and transition dipoles between them. These can be obtained using quantum chemistry approaches. At the end of the laser pulse the quasistatic states $|\mathfrak{n}_t\rangle$ turn into the field-free states $|n\rangle$, which are the eigenvectors of the field-free ionic Hamiltonian.

For the continuum electron, we use an approach similar to the one we have already used for the single-electron problem [4]. For the multichannel case, we define the continuum states as solutions of the channel-specific one-electron TDSE

$$i\big|\dot{\mathbf{k}}_t^n\big\rangle = H_e^n\big|\mathbf{k}_t^n\big\rangle, \qquad (12)$$

where the one-electron Hamiltonian, defined as

$$H_e^n \equiv \langle \mathfrak{n}_t|H^N - H^{N-1}|\mathfrak{n}_t\rangle, \qquad (13)$$

describes the dynamics of the electron in the laser field, the Coulomb potential of the nuclei $V_C(\mathbf{r}) = -\sum_m^{i=N} Z_m/|\mathbf{R}_m - \mathbf{r}|$, and the Hartree potential of the core electrons,

$$V_H^n(t) \equiv \langle \mathfrak{n}_t|V_{ee}|\mathfrak{n}_t\rangle. \qquad (14)$$

The electron-electron operator $V_{ee} \equiv V_{ee}^N - V_{ee}^{N-1}$ describes the Coulomb interaction between the departing electron and all the electrons left in the ion. Note that the Hartree potential [Eq. (14)] is defined for the quasistatic states of the ion and hence includes polarization of the core by the laser field.

In practice, for analytical calculations we approximate $|\mathbf{k}_t^n\rangle$ with channel specific one-electron eikonal-Volkov states [30], as in the one-electron case. The eikonal-Volkov approximation works well for strong-field ionization [31,32] and laser-assisted one-photon XUV ionization [33–35]. These states are obtained by backpropagating field-free continuum solutions defined at a time T after the laser field has been switched off. For large $T \to \infty$, these field-free solutions can be well approximated by plane waves, characterized by a momentum $\mathbf{k}$. Under this assumption, we can express the EVA states at any general time t as

$$\langle \mathbf{r}|\mathbf{k}_n^{EVA}(t)\rangle = \frac{1}{(2\pi)^{3/2}} e^{i(\mathbf{k}+\mathbf{A}(t))\cdot\mathbf{r} - \frac{i}{2}\int_T^t d\tau[\mathbf{k}+\mathbf{A}(\tau)]^2}$$

$$\times e^{-i\int_T^t d\tau U_n(\mathbf{r}_L(\tau;\mathbf{r},\mathbf{k},t))}, \qquad (15)$$

where

$$\mathbf{r}_L(\tau;\mathbf{r},\mathbf{k},t) = \mathbf{r} + \int_t^\tau dt''[\mathbf{k}+\mathbf{A}(t'')] \qquad (16)$$

and U_n is the effective ionic potential experienced by the departing electron in channel n.

By introducing a basis of laser dressed states for the ion and electron, we imply that, in the absence of electron-electron correlation which couples these systems, the laser-induced dynamics can be modeled accurately. While for analytical calculations we use approximate eikonal-Volkov states, the single-electron problem can be solved efficiently and the dynamics of the continuum electron can be accurately described numerically. Bound-state dynamics in the ion are also reasonably simple as long as they require only a limited set of ionic states; that is, the ion can be modeled as a multilevel system in a laser field.

B. Multichannel amplitudes

Having defined the channels, we can now introduce the channel projector:

$$\hat{I} = \int d\mathbf{k} \sum_n \mathbb{A}\big|\mathfrak{n}_t \otimes \mathbf{k}_t^n\big\rangle\big\langle\mathfrak{n}_t \otimes \mathbf{k}_t^n\big|\mathbb{A}. \qquad (17)$$

Here the integration is over all asymptotic momenta $\mathbf{k}$, which characterize each channel-specific continuum state $|\mathbf{k}_t^n\rangle$. Equation (17) implies an (over)complete basis of the quasistatic states for the ion and the active electron, including continuum states of the ion and bound states of the active electron. Operator $\mathbb{A}$ antisymmetrizes electrons and removes basis set overcompleteness [36]. Inserting $\hat{I}$ into Eq. (10) gives a multichannel representation of the time-dependent wave function (omitting the $\otimes$ sign):

$$|\Psi(t)\rangle = -i \sum_n \int d\mathbf{k} \int_{-\infty}^t dt' U^N(t,t')\mathbb{A}\big|\mathfrak{n}_{t'}\mathbf{k}_{t'}^n\big\rangle$$

$$\times \big\langle \mathfrak{n}_{t'}\mathbf{k}_{t'}^n\big|\mathbb{A}\widehat{\Delta}(a)\hat{B}\big|\psi_g^N\big\rangle a_g(t')e^{-iE_g t'}. \qquad (18)$$

Before proceeding further, consider the matrix element determined by the Bloch operator, which is a single-particle operator acting on all N electrons. This matrix element includes two groups of terms. The first group contains those terms where an electron i crossing the boundary $r_i = a$ is projected onto the continuum state, while the other $N-1$ electrons staying inside the inner region are projected onto the ionic state $\mathfrak{n}_{t'}$. The second group includes exchange-like terms, where an electron $j \neq i$ from the inner region is projected onto the continuum state, while the electron i at the boundary is projected onto the bound ionic state. It is straightforward to check that for a sufficiently large radius a of the boundary ($\kappa a \gg 1$), the second group of terms gives an exponentially small contribution compared to the first group.

The equivalence of electrons ensures that all N terms in the first group are identical, and we can label r_1 the electron that leaves the inner region and $i = 2, \ldots, N$ the electrons that stay inside the ion at the moment t'. Recalling the normalization factor $1/\sqrt{N}$ coming from antisymmetrization and introducing channel-specific Dyson orbitals for the quasistatic state of the ion,

$$\big|\mathfrak{n}_{t'}^D\big\rangle = \sqrt{N}\big\langle \mathfrak{n}_{t'}\big|\psi_g^N\big\rangle, \qquad (19)$$

we rewrite Eq. (18) as

$$|\Psi(t)\rangle = -i \sum_n \int d\mathbf{k} \int_{-\infty}^t dt' U^N(t,t') |\mathfrak{n}_{t'} \mathbf{k}_{t'}^n\rangle$$
$$\times \langle \mathbf{k}_{t'}^n | \widehat{\Delta}_1(a) \hat{B}_1 | \mathfrak{n}_{t'}^D \rangle a_g(t') e^{-iE_g t'}. \quad (20)$$

Next, let us turn our attention to the N-electron propagator U^N, which acts on the $N-1$ core electrons and one outgoing electron. Their interaction introduces correlation-induced coupling between the channels. To single out the contribution of these dynamics, for each channel n, we split up our full Hamiltonian (1) as

$$H^N = H_n^N + V_{ee}^n(t). \quad (21)$$

Here, H_n^N is the "correlation-free" Hamiltonian for channel n. It is a sum of the Hamiltonian for the $N-1$ electrons which remain in the ion and the Hamiltonian for the continuum electron moving in the self-consistent field of the core,

$$H_n^N \equiv H^{N-1} + H_e^n. \quad (22)$$

This Hamiltonian fully describes laser-induced dynamics in the ion, as well as the dynamics of the continuum electron in the laser field, the field of the nucleus and the Hartree potential [Eq. (14)] for channel n. However, it ignores coupling between the electrons in the ion and the departing electron. Correspondingly, the propagator $U_n^N(t,t')$ will be a product of the propagator for the continuum electron $U_e^n(t,t')$ and for the ion $U^{N-1}(t,t')$, $U_n^N(t,t') = U^{N-1}(t,t') U_e^n(t,t')$.

The second term,

$$V_{ee}^n(t) \equiv V_{ee} - \langle \mathfrak{n}_t | V_{ee} | \mathfrak{n}_t \rangle, \quad (23)$$

describes correlations between the outgoing electron and the electrons which remain.

With this in mind, we can introduce the following channel-specific Dyson expansion of the full propagator

$$U^N(t,t') = -i \int_{t'}^t dt'' U^N(t,t'') V_{ee}^n(t'') U_n^N(t'',t') + U_n^N(t,t'). \quad (24)$$

This allows us to rewrite the total wave function (20) as a sum of two contributions. The first is the "direct" contribution which does not include electron-electron correlation,

$$|\Psi^{(1)}(T)\rangle = -i \sum_n \int d\mathbf{k} \int^T dt' U^{N-1}(T,t') |\mathfrak{n}_{t'}\rangle$$
$$\times U_e^n(T,t') |\mathbf{k}_{t'}^n\rangle \langle \mathbf{k}_{t'}^n | \widehat{\Delta}_1(a) \hat{B}_1 | \mathfrak{n}_{t'}^D \rangle a_g(t') e^{-iE_g t'}. \quad (25)$$

The second is the "indirect" correlation-driven contribution that we are interested in,

$$|\Psi^{(2)}(T)\rangle = - \sum_n \int d\mathbf{k} \int^T dt'' \int^{t''} dt' U^N(T,t'') V_{ee}^n(t'')$$
$$\times U^{N-1}(t'',t') |\mathfrak{n}_{t'}\rangle U_e^n(t'',t') |\mathbf{k}_{t'}^n\rangle \langle \mathbf{k}_{t'}^n | \widehat{\Delta}_1(a)$$
$$\times \hat{B}_1 | \mathfrak{n}_{t'}^D \rangle a_g(t') e^{-iE_g t'}. \quad (26)$$

IV. DIRECT IONIZATION AMPLITUDES

Let us begin with the first term, Eq. (25). Direct ionization amplitudes are obtained by projecting $|\Psi^{(1)}(T)\rangle$ onto the final states of the continuum electron and the ionic core. However, we should keep in mind that the quasistatic states we have used to define the ionization channels represent a good basis only for a fraction of the laser cycle. They do not include real laser-induced excitations which develop on the time scale of a laser cycle and longer. These transitions can redistribute the amplitude associated with a particular ionization channel between other channels on the time scale of several cycles after the ionization itself has been completed, obscuring the picture.

To obtain meaningful channel-specific direct ionization amplitudes $a_n(\mathbf{p})$, we recall the results obtained for the single-electron case [4]. For a given final momentum $\mathbf{p}$, the integral over time t' has contributions associated with different periodically spaced saddle points $t_s(\mathbf{p})$, where $t_s(\mathbf{p}) = t_i(\mathbf{p}) + i \tau_T(\mathbf{p})$ satisfies

$$(\mathbf{p} + \mathbf{A}(t_s))^2 = -2I_p \quad (27)$$

and I_p is the ionization potential. Each saddle point, associated with some final momentum $\mathbf{p}$, corresponds to a particular ionization burst centered around one of the instantaneous maxima of the oscillating laser field. Ionization is essentially completed when the complex-valued trajectory associated with the saddle point $t' = t_s(\mathbf{p})$ descends to the real time axis. We therefore rewrite the ionic propagator as $U^{N-1}(T,t') = U^{N-1}(T,t_0) U^{N-1}(t_0,t')$. The moment t_0 is selected on the real time axis, ensuring that the saddle-point region around $t_s(\mathbf{p})$ is passed. For the calculations described below, we use $t_0 = \text{Re}[t_s(\mathbf{p})] = t_i$.

We now project the wave function at the moment T onto the ionic basis $U^{N-1}(T,t_0)|\mathfrak{m}_{t_0}\rangle$ and the final state of the continuum electron $|\mathbf{p}\rangle$ to obtain the ionization amplitude associated with the continuum electron with momentum $\mathbf{p}$. Since we are interested only in the contribution of a single ionization burst near t_0 to the total ionization amplitude, we restrict our t' integral to the vicinity of a single saddle point $t_s(\mathbf{p})$ by introducing the contour $C(\mathbf{p},t_0)$. This fact is stressed by keeping t_0 in the argument of $a_{mn}^{(1)}(\mathbf{p},t_0)$:

$$a_{mn}^{(1)}(\mathbf{p},t_0) = -i \int d\mathbf{k} \int_{C(\mathbf{p},t_0)} dt' \langle \mathfrak{m}_{t_0} | U^{N-1}(t_0,t') | \mathfrak{n}_{t'}\rangle$$
$$\times \langle \mathbf{p} | U_e^n(T,t') | \mathbf{k}_{t'}^n \rangle \langle \mathbf{k}_{t'}^n | \widehat{\Delta}_1(a) \hat{B}_1 | \mathfrak{n}_{t'}^D \rangle a_g(t') e^{-iE_g t'}. \quad (28)$$

Note that this amplitude correlates to the final state of the ion $|\widetilde{m}(T,t_0)\rangle = U^{N-1}(T,t_0)|\mathfrak{m}_{t_0}\rangle$, where $|\widetilde{m}(T,t_0)\rangle$ is some superposition of field-free states. The amplitude is formed by the time t_0. From t_0 to T, only phase is accumulated in the matrix element $\langle \mathbf{p} | U_e^n(T,t') | \mathbf{k}_{t'}^n \rangle$ (up to a nonadiabatic Coulomb correction, discussed in [4], which is unimportant for ionization near the peak of the laser field), accompanied by unitary evolution of the ion $U^{N-1}(T,t_0)|\mathfrak{m}_{t_0}\rangle$.

Equation (28) accounts for the fact that the laser field can induce transitions between different quasistatic states during the time interval $t_0 - t_s(\mathbf{p})$. However, in all cases considered below, such transitions are negligible during the short time interval $t_0 - t_s(\mathbf{p})$. One can therefore use the quasistatic

approximation for the short-time propagator $U^{N-1}(t_0,t')$ and the matrix elements $\langle \mathfrak{m}_{t_0} | U^{N-1}(t_0,t') | \mathfrak{n}_{t'} \rangle$:

$$
\begin{aligned}
\langle \mathfrak{n}_{t_0} | U^{N-1}(t_0,t') | \mathfrak{m}_{t'} \rangle &= \delta_{mn} b_m(t_0,t') e^{-iE_m(t_0-t')} \\
&= \delta_{mn} e^{-i\int_{t'}^{t_0} \Delta E_m^{(\text{St})}(\tau)d\tau - iE_m(t_0-t')}. \quad (29)
\end{aligned}
$$

Here E_m is the field-free energy of the ionic state $|m\rangle$. The additional factor $b_m(t_0,t')$ accounts for the quasistatic Stark shift $\Delta E_m^{(\text{St})}(\tau)$.

In practice (see Sec. VI), we will not make the quasistatic approximation when calculating the matrix element Eq. (29). However, off-diagonal contributions will be negligible. The diagonal contribution is

$$
\begin{aligned}
a_{nn}^{(1)}(\mathbf{p},t_0,T) &= -i \int d\mathbf{k} \int_{C(\mathbf{p},t_0)} dt' b_n(t_0,t') e^{-iE_n(t_0-t')} \\
&\quad \times \langle \mathbf{p} | U_e^n(T,t') | \mathbf{k}_{t'}^n \rangle \langle \mathbf{k}_{t'}^n | \widehat{\Delta}_1(a) \hat{B}_1 | \mathfrak{n}_{t'}^D \rangle a_g(t') \\
&\quad \times e^{-iE_g t'}. \quad (30)
\end{aligned}
$$

Orthogonality of the continuum states $|\mathbf{k}_{t'}^n\rangle$ means that this expression simplifies to

$$
\begin{aligned}
a_{nn}^{(1)}(\mathbf{p},t_0,T) &= -i \int_{C(\mathbf{p},t_0)} dt' b_n(t_0,t') e^{-iE_n(t_0-t')} \\
&\quad \times \langle \mathbf{p}_{t'}^n | \widehat{\Delta}_1(a) \hat{B}_1 | \mathfrak{n}_{t'}^D \rangle a_g(t') e^{-iE_g t'}. \quad (31)
\end{aligned}
$$

The amplitude $a_{nn}^{(1)}(\mathbf{p})$ is very similar to the single active electron (SAE) case (see, e.g., our companion paper [4]). The difference is the extra phase evolution in the ionic channel n. First, it encodes the field-free ionization potential for this channel,

$$
I_{p,n} = E_n - E_g. \quad (32)
$$

Second, the Stark shifts of both neutral and ionic states are also present, via $a_g(t')$ and $b_n(t_0,t')$, respectively. Treating both $a_g(t')$ and $b_n(t_0,t')$ as slow functions and evaluating the t' integral using the saddle-point method, we can express the ionization amplitude $a_{nn}^{(1)}$ via its SAE counterpart a_{SAE},

$$
a_{nn}^{(1)}(\mathbf{p},t_0) = a_g(t_s) b_n(t_0,t_s) e^{-iE_n t_0} a_{\text{SAE}}(\mathbf{p}; I_{p,n}, t_0). \quad (33)
$$

Note that in our companion paper [4], $a_g(t_s)$ was included in a_{SAE}. The role of the ground-state wave function in the single-electron ionization amplitude is played by the Dyson orbital for the channel, and the unperturbed ionization potential is $I_{p,n}$. Both amplitudes refer to the contribution of a single ionization burst around $t_0 = \text{Re } t_s(\mathbf{p})$.

V. CORRELATION-DRIVEN INDIRECT IONIZATION AMPLITUDES

Consider now the correlation-driven contribution to the total wave function:

$$
\begin{aligned}
|\Psi^{(2)}(T)\rangle &= -\sum_n \int d\mathbf{k} \int^T dt'' \int^{t''} dt' U^N(T,t'') V_{ee}^n(t'') \\
&\quad \times U^{N-1}(t'',t') | \mathfrak{n}_{t'} \rangle U_e^n(t'',t') | \mathbf{k}_{t'}^n \rangle \langle \mathbf{k}_{t'}^n | \widehat{\Delta}_1(a) \\
&\quad \times \hat{B}_1 | \mathfrak{n}_{t'}^D \rangle a_g(t') e^{-iE_g t'}. \quad (34)
\end{aligned}
$$

In this exact expression, propagation between t' and t'' is correlation-free, but includes the effect of the self-consistent

field of the core on the outgoing electron. Correlation can induce transitions at an instant moment t'', after which the full propagator is applied.

Let us now project this wave function onto the ionic basis $U^{N-1}(T,t_0)|\mathfrak{m}_{t_0}\rangle$ and the final state of the continuum electron $|\mathbf{p}\rangle$ at time T, just as we did for the direct channel. To first order in electron-electron correlation, we can approximate the full propagator after t'' as

$$
U^N(T,t'') \simeq U^{N-1}(T,t'') U_e^m(T,t''). \quad (35)
$$

Doing this, we obtain the correlation-induced transition amplitude from the quasistatic ionic state n to the quasistatic state m:

$$
\begin{aligned}
a_{mn}^{(2)}(\mathbf{p},t_0) &= -\int d\mathbf{k} \int^{t_0} dt'' \int^{t''} dt' \langle \mathbf{p}_{t''}^m | \langle \mathfrak{m}_{t_0} | U^{N-1}(t_0,t'') \\
&\quad \times | V_{ee}^n(t'') U^{N-1}(t'',t') | \mathfrak{n}_{t'} \rangle | \mathbf{k}_{t''}^n \rangle \langle \mathbf{k}_{t'}^n | \widehat{\Delta}_1(a) \\
&\quad \times \hat{B}_1 | \mathfrak{n}_{t'}^D \rangle a_g(t') e^{-iE_g t'}. \quad (36)
\end{aligned}
$$

Here, we have again restricted our time integral by setting the upper limit of the t'' integral to t_0. This allows us to compute the contribution from a particular ionization burst as the continuum electron is moving away and eliminates the contribution of the electron-ion recollision which happens after the laser field turns the outgoing electron around and brings it back to the core. Such contributions, responsible for nonsequential double ionization [37], are described by an equation similar to Eq. (36), except that the corresponding contribution to the t'' integral comes from later times $t'' > t_0$, separated from t_0 by about half a laser cycle or more. Restricting the inner (i.e., t') integral to the vicinity of a single saddle point effectively sets the lower limit of the outer t'' integral to $t_s(\mathbf{p})$.

Finally, let us explicitly factor out the phases associated with the channel energies,

$$
\begin{aligned}
U^{N-1}(t'',t') | \mathfrak{n}_{t'} \rangle &= e^{-iE_n(t''-t')} b_n(t'',t') | \mathfrak{n}(t'',t') \rangle, \\
\langle \mathfrak{m}_{t_0} | U^{N-1}(t_0,t'') &= e^{-iE_m(t_0-t'')} b_m(t_0,t'') \langle \mathfrak{m}(t_0,t'') |,
\end{aligned} \quad (37)
$$

where slow functions b_k incorporate Stark shifts of the quasistatic channels. Note that states $|\mathfrak{n}(t'',t')\rangle$ and $|\mathfrak{m}(t'',t_0)\rangle$ defined by the above equations may be superpositions of different quasistatic states. With this notation, we get

$$
\begin{aligned}
a_{mn}^{(2)}(\mathbf{p},t_0) &= -\int d\mathbf{k} \int^{t_0} dt'' \int^{t''} dt' b_m(t_0,t'') e^{-iE_m(t_0-t'')} \\
&\quad \times \langle \mathfrak{m}(t_0,t'') | \langle \mathbf{p}_{t''}^m | V_{ee}^n(t'') | \mathfrak{n}(t'',t') \rangle | \mathbf{k}_{t''}^n \rangle b_n(t'',t') \\
&\quad \times e^{-iE_n(t''-t')} \langle \mathbf{k}_{t'}^n | \widehat{\Delta}_1(a) \hat{B}_1 | \mathfrak{n}_{t'}^D \rangle a_g(t') e^{-iE_g t'}. \\
&\qquad\qquad\qquad\qquad\qquad\qquad\qquad\qquad\qquad\qquad (38)
\end{aligned}
$$

The integral over t', as we will soon see, is again accumulated near the saddle point $t_s(\mathbf{p})$. Pre-empting this, for convenience of notation, we can therefore take the slow function $b_n(t'',t')$ out of the t' integral at the saddle point, replacing it with $b_n(t'',t_s)$. The same is done with $|\mathfrak{n}(t'',t')\rangle$. Recalling that $V_{ee}^n = V_{ee}^n(\mathbf{r},\ldots,\mathbf{r}_N)$ and inserting the identity on the coordinates of the departing electron, $\int d\mathbf{r}|\mathbf{r}\rangle\langle\mathbf{r}|$, we can rewrite

Eq. (38) as

$$
\begin{aligned}
a_{mn}^{(2)}&(\mathbf{p},t_0)\\
&= -i \int^{t_0} dt'' e^{-iE_m t_0} b_m(t_0,t'') b_n(t'',t_s) e^{i(E_m - E_n)t''}\\
&\quad \times \int d\mathbf{r} \int d\mathbf{k} \, \langle \mathbf{p}_{t''}^m | \mathbf{r}\rangle \, \langle \mathfrak{m}(t_0,t'')| V_{ee}^n(t'',\mathbf{r})|\mathfrak{n}(t'',t_s)\rangle \langle \mathbf{r} | \mathbf{k}_{t''}^n\rangle\\
&\quad \times \left[(-i)\int^{t''} dt' \langle \mathbf{k}_{t'}^n | \hat{\Delta}_1(a)\hat{B}_1 | \mathfrak{n}_{t'}^D\rangle \, a_g(t') e^{iI_{p,n}t'}\right].
\end{aligned} \tag{39}
$$

The operator $V_{ee}^n(t'',\mathbf{r})$ in Eq. (39) acts on all electrons but the notation explicitly stresses the coordinate $\mathbf{r}$ of the outgoing electron.

The expression in square brackets in Eq. (39) is almost exactly the SAE ionization amplitude $a_{\mathbf{k}}(T)$, which we calculated in the companion paper [4], with the hydrogen bound state replaced by a Dyson orbital $|\mathfrak{n}_{t'}^D\rangle$. The main difference here is that the upper limit of the t' integral is t''; the form of the t' integrand itself is identical. However, as we saw in [4] and as we discussed for the direct channel, the contribution to the integral over t' comes only from the saddle-point region $t_s(\mathbf{p})$, determined by Eq. (27). Thus, assuming we choose the contour for t'' appropriately, this upper limit should not affect the value of our integral. We can therefore replace the expression in square brackets by $a_{\mathbf{k}}(T)$,

$$
\begin{aligned}
a_{mn}^{(2)}(\mathbf{p},t_0) &= -i \int^{t_0} dt'' e^{-iE_m t_0} b_m(t_0,t'') b_n(t'',t_s) e^{i(E_m - E_n)t''}\\
&\quad \times V_{mn}(\mathbf{p},t''),
\end{aligned} \tag{40}
$$

where we have introduced

$$
\begin{aligned}
V_{mn}(\mathbf{p},t'') &= \int d\mathbf{r} \int d\mathbf{k} \, \langle \mathfrak{m}(t_0,t'')| V_{ee}^n(t'',\mathbf{r})|\mathfrak{n}(t'',t_s)\rangle\\
&\quad \times \langle \mathbf{p}_{t''}^m | \mathbf{r}\rangle \langle \mathbf{r} | \mathbf{k}_{t''}^n\rangle \, a_{\mathbf{k}}(T).
\end{aligned} \tag{41}
$$

Let us now look more closely at the integrals over $\mathbf{k}$ and $\mathbf{r}$ above. To evaluate these explicitly, we use eikonal-Volkov states (15) for $\langle \mathbf{p}_{t''}^m | \mathbf{r}\rangle$ and $\langle \mathbf{r} | \mathbf{k}_{t''}^n\rangle$ and quote the following analytical result for $a_{\mathbf{k}}(T)$ from [4]:

$$
\begin{aligned}
a_{\mathbf{k}}(T) &= a_g(t_s) R_n(\mathbf{k}) e^{-\frac{i}{2}\int_{t_s}^T d\tau [\mathbf{k}+\mathbf{A}(\tau)]^2 + iI_p t_s}\\
&\quad \times e^{-i\int_{t_\kappa}^T d\tau U\left(\int_{t_s}^\tau dt'[\mathbf{k}+\mathbf{A}(t'')]\right)}.
\end{aligned} \tag{42}
$$

Here, $R_n(\mathbf{k})$ is a term that encodes the impact of the angular structure of our channel-n Dyson orbital on ionization exactly as $R_{\kappa lm}(\mathbf{k})$ did for hydrogen bound states in [4]. The implementation for calculating $R_n(\mathbf{k})$ terms here will be analogous to the one discussed by Murray *et al.* for static fields [38], showing how the static approach extends to oscillating fields.

Substituting in these expressions, we obtain

$$
\begin{aligned}
V_{mn}(\mathbf{p},t'') &= e^{-i/2\int_{t''}^T(\mathbf{p}+A(\tau))^2 d\tau} \frac{1}{(2\pi)^3}\int d\mathbf{r}\\
&\quad \times \int d\mathbf{k} \, e^{i(\mathbf{k}-\mathbf{p})\cdot\mathbf{r}} \, e^{-i/2\int_{t_s}^{t''}(\mathbf{k}+A(\tau))^2 d\tau} e^{iI_{p,n}t_s}\\
&\quad \times a_g(t_s) R_n(\mathbf{k}) \, \langle \mathfrak{m}(t_0,t'')| V_{ee}^n(t'',\mathbf{r})|\mathfrak{n}(t'',t_s)\rangle\\
&\quad \times e^{-iW_c^{mn}(t'',\mathbf{r},\mathbf{k},T)},
\end{aligned} \tag{43}
$$

where

$$
\begin{aligned}
W_c^{mn}(t'',\mathbf{r},\mathbf{k},T) &= \int_{t''}^T d\tau \, U_m\left(\mathbf{r}+\int_{t''}^\tau d\zeta[\mathbf{p}+\mathbf{A}(\zeta)]\right)\\
&\quad + \int_T^{t''} d\tau \, U_n\left(\mathbf{r}+\int_{t''}^\tau d\zeta[\mathbf{k}+\mathbf{A}(\zeta)]\right)\\
&\quad + \int_{t_\kappa}^T d\tau \, U_n\left(\int_{t_s}^\tau d\zeta[\mathbf{k}+\mathbf{A}(\zeta)]\right).
\end{aligned} \tag{44}
$$

If we now compare this to $a_{\mathbf{p}}(t)$ in [4], we see that the integrals we have to evaluate are entirely analogous. We have simply gained the factor $\langle \mathfrak{m}(t_0,t'')| V_{ee}^n(t'',\mathbf{r})|\mathfrak{n}(t'',t_s)\rangle$, and W_c now has an additional U_m-dependent term. Both these terms, however, can be treated as slow prefactors and will not affect our saddle-point analysis. Thus, following the derivation in [4], we shall proceed by integrating first over $\mathbf{k}$ and then over $\mathbf{r}$.

Applying the saddle-point method for the integral over $\mathbf{k}$, assuming that $R_n(\mathbf{k})$ is slowly varying and well-behaved, we find

$$
\begin{aligned}
V_{mn}(\mathbf{p},t'') &\simeq e^{-i/2\int_{t''}^T(\mathbf{p}+A(\tau))^2 d\tau}\int d\mathbf{r}\, \frac{e^{-i\pi/4}}{[2\pi(t''-t_s)]^{3/2}}\\
&\quad \times e^{\frac{i}{2}\frac{(\mathbf{r}-\mathbf{r}_s(\mathbf{p},t''))^2}{t''-t_s}} e^{-i/2\int_{t_s}^{t''}(\mathbf{p}+A(\tau))^2 d\tau} e^{iI_{p,n}t_s}\\
&\quad \times a_g(t_s) R_n(\mathbf{k}_s) \, \langle \mathfrak{m}(t_0,t'')| V_{ee}^n(t'',\mathbf{r})|\mathfrak{n}(t'',t_s)\rangle\\
&\quad \times e^{-iW_c^{mn}(t'',\mathbf{r},\mathbf{k}_s,T)},
\end{aligned} \tag{45}
$$

where the stationary momentum $\mathbf{k}_s$ is given by

$$
\mathbf{k}_s = \frac{\mathbf{r}-\int_{t_s}^{t''}\mathbf{A}(\tau)d\tau}{t''-t_s}, \tag{46}
$$

and

$$
\mathbf{r}_s(\mathbf{p},t'') = \int_{t_s}^{t''}[\mathbf{p}+\mathbf{A}(\tau)]d\tau. \tag{47}
$$

The presence of the wave packet $\exp[\frac{i}{2}\frac{(\mathbf{r}-\mathbf{r}_s(\mathbf{p},t''))^2}{t''-t_s}]/[2\pi(t''-t_s)]^{3/2}$ above allows us to evaluate the $\mathbf{r}$ integral using the saddle-point method, where the saddle point is given by Eq. (47) above. Note that in the classically forbidden region $t''-t_s = -i\xi$, this wave packet becomes a Gaussian. It is the presence of this term which allows us to use a single tunneling trajectory, as defined by Eq. (47), to evaluate the contribution of the core potential to the SAE ionization amplitude $a_{\mathbf{p}}(t)$ in [4]. For exactly the same reason, we can also substitute it in the correlation-driven matrix element $\langle \mathfrak{m}(t_0,t'')| V_{ee}^n(\mathbf{r})|\mathfrak{n}(t'',t_s)\rangle$ here. Doing this, and noting that Eqs. (46) and (47) together imply $\mathbf{k}_s = \mathbf{p}$, we obtain the final result

$$
\begin{aligned}
V_{mn}(\mathbf{p},t'') &\simeq a_g(t_s) R_n(\mathbf{p}) \, e^{-i/2\int_{t_s}^T(\mathbf{p}+A(\tau))^2 d\tau} e^{iI_{p,n}t_s}\\
&\quad \times \langle \mathfrak{m}(t_0,t'')| V_{ee}^n(\mathbf{r}_s(t''))|\mathfrak{n}(t'',t_s)\rangle\\
&\quad \times e^{-i\int_{t''}^T d\tau \, U_m(\mathbf{r}_s(\mathbf{p},\tau))} e^{-i\int_{t_\kappa}^{t''} d\tau \, U_n(\mathbf{r}_s(\mathbf{p},\tau))}.
\end{aligned} \tag{48}
$$

Introducing the correction factor,

$$
Q_{mn}(t'') \equiv \int_{t''}^T d\tau \, [U_m(\mathbf{r}_s(\tau)) - U_n(\mathbf{r}_s(\tau))], \tag{49}
$$

we can express this as

$$
V_{mn}(\mathbf{p},t'') \simeq \left[a_g(t_s) R_n(\mathbf{p}) \, e^{-i/2 \int_{t_s}^{T} (\mathbf{p}+A(\tau))^2 d\tau} \, e^{i I_{p,n} t_s} \right.
$$
$$
\left. \times \, e^{-i \int_{t_\kappa}^{T} d\tau \, U_n(\mathbf{r}_s(\mathbf{p},\tau))} \right] \langle \mathfrak{m}(t_0,t'') | V_{ee}^n(\mathbf{r}_s(t''))
$$
$$
\times \, | \mathfrak{n}(t'',t_s) \rangle \, e^{-i Q_{mn}(t'')}. \tag{50}
$$

Comparing the first term [in brackets] to Eq. (42), we see that this is simply the SAE ionization amplitude for channel n, $a_{\mathbf{p}}(T) = a_g(t_s) \, a_{\text{SAE}}(\mathbf{p}; I_{p,n}, t_0)$. Thus, we can now write down a simple expression for our correlation-driven multichannel ionization amplitude:

$$
a_{mn}^{(2)}(\mathbf{p},t_0) = -i \int^{t_0} dt'' e^{-i E_m t_0} b_m(t_0,t'') b_n(t'',t_s) e^{i(E_m - E_n) t''}
$$
$$
\times \, a_g(t_s) a_{\text{SAE}}(\mathbf{p}; I_{p,n}, t_0) \langle \mathfrak{m}(t_0,t'') | V_{ee}^n(\mathbf{r}_s(t''))
$$
$$
\times \, | \mathfrak{n}(t'',t_s) \rangle \, e^{-i Q_{mn}(t'')}. \tag{51}
$$

Recalling our final result for the direct channel ionization amplitude Eq. (33), we can express this as

$$
a_{mn}^{(2)}(\mathbf{p},t_0) = c_{mn}(t_0,t_s) \, b_n^{-1}(t_0,t_s) \, a_{nn}^{(1)}(\mathbf{p},t_0), \tag{52}
$$

where

$$
c_{mn}(t_0,t_s) = -i \int_{t_s}^{t_0} dt'' \langle \mathfrak{m}_{t_0} | U^{(N-1)}(t_0,t'') V_{ee}^n(\mathbf{r}_s(t''))
$$
$$
\times \, U^{(N-1)}(t'',t_s) | \mathfrak{n}_{t_s} \rangle \, e^{-i Q_{mn}(t'')} \tag{53}
$$

or, explicitly writing out phases associated with the unperturbed energies of the channels,

$$
c_{mn}(t_0,t_s) = -i \int_{t_s}^{t_0} dt'' b_m(t_0,t'') b_n(t'',t_s) e^{-i(E_m - E_n)(t_0 - t'')}
$$
$$
\times \, \langle \mathfrak{m}(t_0,t'') | V_{ee}^n(\mathbf{r}_s(t'')) | \mathfrak{n}(t'',t_s) \rangle \, e^{-i Q_{mn}(t'')}. \tag{54}
$$

Note that both t_s and $t_0 = \text{Re}[t_s]$ are determined by the momentum $\mathbf{p}$.

The amplitude c_{mn} describes correlation-induced transitions between the quasistatic electronic states of the ion. The field responsible for these transitions is created by the departing electron, which arrives at the detector with momentum $\mathbf{p}$. The transitions occur while the tunneling electron is moving away from the core via the classically forbidden region and result in correlation-driven ionization into channel m.

The evolution of the states $\langle \mathfrak{m}(t_0,t'') |$ and $| \mathfrak{n}(t'',t_s) \rangle$ is exact. The t'' integral is taken in complex time, from the saddle point $t_s = t_0 + i \tau_T(\mathbf{p})$ to $t_0 = \text{Re}(t_s)$. Consequently, $t_0 - t'' = -i\xi$ and the factor $\exp(-i(E_m - E_n)(t_0 - t''))$ in the integrand becomes $\exp(-(E_m - E_n)\xi)$. This results in the exponential suppression of the excitation amplitude $c_{mn}(\mathbf{p})$ if the eigenstate $|m\rangle$ has higher energy than the eigenstate $|n\rangle$ [39], that is, $\Delta I_p \equiv E_m - E_n > 0$.

Consider ionization at the maximum of the instantaneous laser field, when $\mathbf{p}/v_0 = \mathbf{p}/\sqrt{4 U_p} \simeq 0$, with $U_p = F^2/4\omega^2$ the ponderomotive potential. In this case $t_s = i\tau_T$ and $t_0 = 0$. Changing the integration variable to imaginary $\xi = i(t_0 - t'')$, we see that when the laser-induced Stark shifts in the ion and the difference between the core potentials for different

ionization channels are neglected, we have

$$
c_{mn} = \int_{\tau_T}^{0} d\xi \, e^{-\Delta I_p \xi} \langle m | V_{ee}^n(\mathbf{r}_s(\xi)) | n \rangle. \tag{55}
$$

This expression shows that the exponential suppression factor $e^{-\Delta I_p \xi}$ favors excitation which occurs close to the exit from the tunnel ($\xi = 0$). The role of this factor is discussed in our short report [40].

It will be convenient to evaluate the strength of the indirect channel $n \to m$ by normalizing the corresponding amplitude with respect to the direct ionization amplitude associated with the "parent" channel n. Using the results above, this ratio is

$$
\widetilde{a}_{mn}^{(2)}(\mathbf{p}) = a_{mn}^{(2)}(\mathbf{p})/a_{nn}^{(1)}(\mathbf{p})
$$
$$
= c_{mn}(t_0,t_s)/b_n(t_0,t_s) \equiv c_{mn}(\mathbf{p})/b_n(\mathbf{p}), \tag{56}
$$

where in the last equality we have stressed that both t_s and $t_0 = \text{Re}[t_s]$ are determined by the final momentum $\mathbf{p}$.

VI. RESULTS

The central result of this work is given by Eqs. (52)–(54), which connect the correlation-induced indirect ionization amplitude with the amplitude for direct ionization from the parent channel. In this section, we analyze the role of the correlation-induced channel in strong-field ionization of N_2 and CO_2 molecules. As we will see, this depends strongly on the electronic structure of the molecule and the details of the laser field parameters. Direct ionization amplitudes are calculated using the analytical approach developed in Refs. [38,41]. We include the effect of Stark shifts, encoded in the direct ionization amplitude via coefficients b_n. Other approaches supplying single-channel ionization amplitudes [28,42,43] could also be used for this purpose.

As an example we consider the contribution to ionization from the instantaneous maximum $t = 0$ of the laser field $F(t) = F_0 \cos(\omega t)$, leading to $\mathbf{p} \simeq 0$. We neglect the correction factor $e^{-i Q_{mn}}$ throughout.

To begin with, consider the case when only two ionic states are involved. Denoting the relevant quasistatic states as $|1\rangle$ and $|2\rangle$, the expressions for c_{mn} and b_n become

$$
c_{21}(\mathbf{p}=0) = \int_{\tau_T}^{0} d\xi \langle 2 | U^{N-1}(0,\xi) V_{ee}^1(\mathbf{r}_s(\xi)) U^{N-1}(\xi,\tau_T) | 1 \rangle,
$$
$$
b_1(\tau_T) = \langle 1 | U^{N-1}(0,\tau_T) | 1 \rangle. \tag{57}
$$

Physically, such a system could describe N_2 aligned at $90°$, where essentially only two states are coupled by the laser field: the ground state $X(X^2 \Sigma_g)$ and the first excited state $A(A^2 \Pi_u)$ separated from the ground state by 1.3 eV. Here, the correlation-driven excitation channel corresponds to the ionic state changing from X to A during ionization.

In order to calculate the amplitude for correlation-induced excitation at (imaginary) time ξ, it is necessary to propagate state $|1\rangle$ in (imaginary) time from $t_s = i\tau_T$ to $t'' = i\xi$ and state $\langle 2 |$ from $t_0 = 0i$ to $t'' = i\xi$:

$$
U^{N-1}(i\xi, i\tau_T) | 1 \rangle = \alpha_{11}(\xi) | X \rangle + \alpha_{21}(\xi) | A \rangle, \tag{58}
$$

$$
\langle 2 | U^{N-1}(0, i\xi) = [\langle X | \beta_{21}^*(\xi) + \langle A | \beta_{22}^*(\xi)] e^{-\Delta I_p^{XA} \xi}. \tag{59}
$$
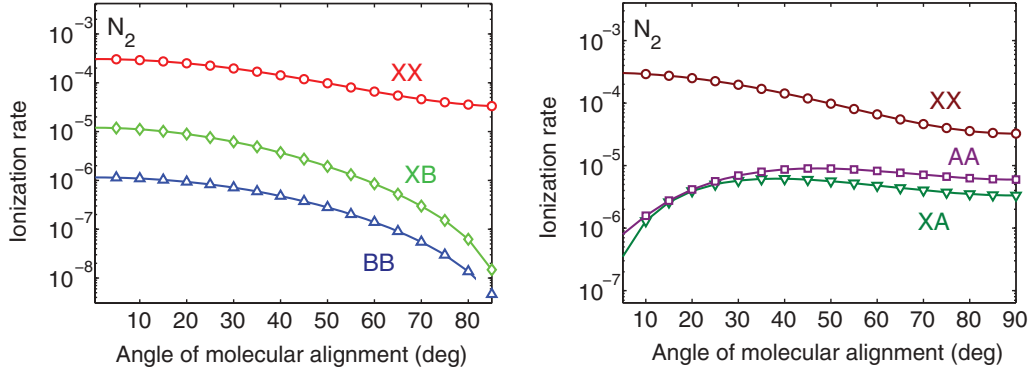
FIG. 2. (Color online) Molecular alignment-dependent ionization rates for direct XX (red circles), AA (violet squares), BB (blue triangles) and correlation-driven channels XB (a) (green diamonds) and XA (b) (green inverted triangles) in N_2. Laser parameters are in the regime of nonadiabatic tunneling ($\gamma \geqslant 1$): $\lambda = 800$ nm, $I = 0.8 \times 10^{14}$ W/cm^2.

Here the amplitudes $\alpha_{ij}(\xi)$, $\beta_{ij}(\xi)$ reflect the time-dependent evolution in the basis of field-free ionic states $|A\rangle$, $|X\rangle$, due to propagation in the laser field. The field-free energies of the two levels are set to $E_X = 0$ and $E_A = \Delta I_p^{XA}$, where $\Delta I_p^{XA} > 0$ is the field-free difference in ionization potentials for channels X and A. Initial conditions for forward and backward propagation in Eqs. (58) and (59) are determined by the projection of the quasistatic eigenstate $|1_{t_s}^{qs}\rangle$ at time $t_s = i\tau_T$ and eigenstate $|2_0^{qs}\rangle$ at time $t_i = 0$ onto the field-free states: $\alpha_{11}(\tau_T) = \langle X|1_{i\tau_T}^{qs}\rangle$, $\alpha_{21}(\tau_T) = \langle A|1_{i\tau_T}^{qs}\rangle$, $\beta_{22}^*(0) = \langle 2_0^{qs}|A\rangle$, $\beta_{21}^*(0) = \langle 2_0^{qs}|X\rangle$. In Eq. (57) the transition between quasistatic states occurs at (imaginary) time ξ. Using Eqs. (58) and (59), the integrand in Eq. (57) can be simplified to yield a "polarized" correlation potential $V_{21}(\xi)$, calculated between the laser-dressed states of the ion:

$$V_{21}(\xi) = \beta_{21}^* \langle X|V_{ee}|X\rangle \alpha_{11} + \beta_{22}^* \langle A|V_{ee}|X\rangle \alpha_{11}$$
$$+ \beta_{21}^* \langle X|V_{ee}|A\rangle \alpha_{21} + \beta_{22}^* \langle A|V_{ee}|A\rangle \alpha_{21}, \quad (60)$$

$$c_{21}(\mathbf{k}_f) = \int_{\tau}^0 d\xi \, V_{21}(\xi) e^{-\Delta I_p^{XA} \xi}. \quad (61)$$

Here all time-dependent amplitudes α_{ij}, β_{ij} are taken at imaginary time $i\xi$. If the states of the ion are not coupled by the laser field ($\alpha_{21} = 0$, $\beta_{21}^* = 0$, $\alpha_{11} = 1$, $\beta_{22}^* = 1$), only the second term $\beta_{22}^* \langle A|V_{ee}|X\rangle \alpha_{11} \equiv \langle A|V_{ee}|X\rangle$, corresponding to the field-free correlation potential, contributes.

The dependence of polarized and field-free correlation potentials for N_2 and CO_2 on the alignment and electronic structure of the molecule has been discussed in our short report [40]. Here we focus on the comparison of direct and indirect pathways which leave the ion in an excited state.

The vertical ionization potential for channels X, A, and B (corresponding to the ion left in the ground and first and second excited electronic states, respectively) are known spectroscopically: 15.6, 16.9, and 19.1 eV for N_2 and 13.8, 17.3, and 18.1 eV for CO_2. To calculate the effects of the laser field, we use complete active space self-consistent field (CASSCF) values for the dipole matrix elements calculated by S. Patchkovskii for these molecules in our previous works [21,24]. For N_2, the dipole coupling vectors between the ionic states are $d_{XA}^{CAS} = (0.25, 0, 0)$, $d_{XB}^{CAS} = (0, 0, 0.72)$, while for CO_2, they are $d_{XA}^{CAS} = (0, 0, 0.46)$, $d_{XB}^{CAS} = (0.27, 0, 0)$. The first component in the brackets is perpendicular and the last is
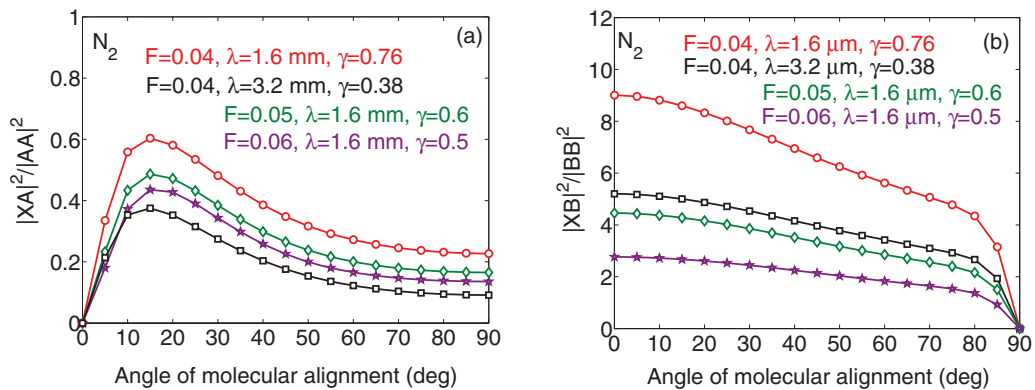
FIG. 3. (Color online) The ratio of ionization rates for correlation-driven and corresponding direct channels leading to the production of N_2^+ ions in excited states A (a) and B (b) for different laser parameters in the tunneling regime ($\gamma < 1$). (a) $F = 0.04$ a.u., $\lambda = 1.6$ μm (red circles); $F = 0.04$ a.u., $\lambda = 3.2$ μm (black squares); $F = 0.05$ a.u., $\lambda = 1.6$ μm (green diamonds); $F = 0.06$ a.u., $\lambda = 1.6$ μm (violet stars). (b) $F = 0.04$ a.u., $\lambda = 1.6$ μm (red circles); $F = 0.04$ a.u., $\lambda = 3.2$ μm (black squares); $F = 0.05$ a.u., $\lambda = 1.6$ μm (green diamonds); $F = 0.06$ a.u., $\lambda = 1.6$ μm (violet stars).
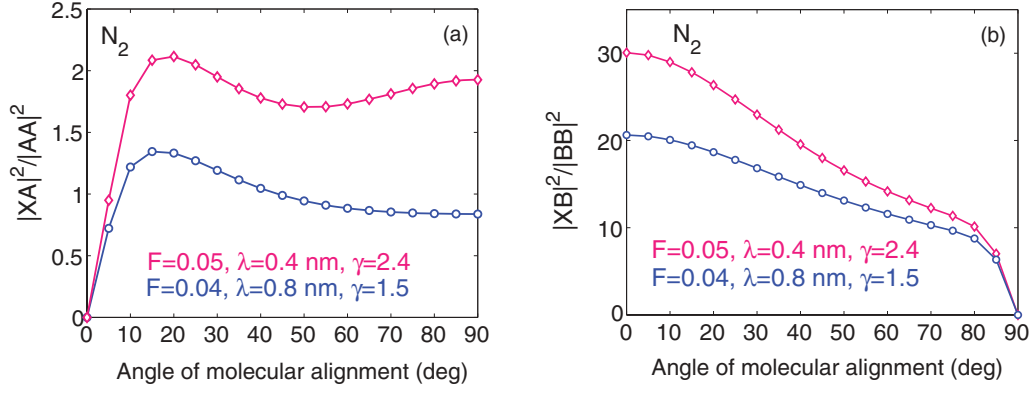
FIG. 4. (Color online) The ratio of ionization rates for correlation-driven and corresponding direct channels leading to the production of N_2^+ ions in excited states A (a) and B (b), for different laser parameters in the regime of nonadiabatic tunneling ($\gamma \geqslant 1$). (a) $F = 0.05$ a.u., $\lambda = 0.4$ μm (pink diamonds); $F = 0.04$ a.u., $\lambda = 0.8$ μm (blue circles). (b) $F = 0.05$ a.u., $\lambda = 0.4$ μm (pink diamonds); $F = 0.04$ a.u., $\lambda = 0.8$ μm (blue circles).

parallel to the molecular axis. It is important to use the more accurate dipoles, because the Hartree-Fock approximation overestimates the strength of the dipole couplings: for the XA transition in CO_2 by a factor of 3.5, for the XB transition in N_2 by a factor of 2.2. Hartree-Fock dipoles would thus overestimate laser-induced dynamics in our molecular ions.

When calculating correlation potentials, here we use the Hartree-Fock orbitals of the neutral molecules. The correlation potential calculated using these orbitals,

$$V_{mn}^{ee}(t) = \int d\mathbf{r} \frac{\phi_m^*(\mathbf{r})\phi_n(\mathbf{r})}{|\mathbf{r}_s(t) - \mathbf{r}|}, \quad n,m = \text{X, A, B}, \quad (62)$$

approaches $V_{mn}^{ee}(t) \approx d_{mn}/r_s^2$ for large r_s, where d_{mn} are the Hartree-Fock dipoles. Thus, it is likely that the unadjusted correlation potential will lead to an overestimation of the correlation effects. This overestimation of the electronic coupling strength is likely to affect any method based on the expectation values of the Hartree Fock orbitals, and may be responsible for the strong laser-induced coupling between the X and A channels in CO_2 reported in Ref. [28]. To correct this problem, we scale the value of the correlation potential by the ratio of the CASSCF and Hartree Fock dipoles; using the full CASSCF correlation potentials is the planned next step.

To calculate angle-resolved ionization rates for the direct ionization channels, we use analytical formulas derived by Murray and Ivanov [38,41]. The Stark shifts of the neutral molecule and of the ion are included in the same way as in our previous work [21,24].

As correlation-driven excitation is not subject to the full exponential suppression characteristic of direct ionization from lower orbitals, it becomes particularly important for low fields and high $\Delta I_p \tau$, that is, in the regime of nonadiabatic tunneling. However, our results indicate that this channel is also important in the tunneling regime $\gamma < 1$.

We first consider N_2, where correlation-driven channels are particularly strong. We treat the N_2^+ ion as a three-level system, in the same manner as the two-level system discussed earlier. The correlation potentials are

$$V_{\mathfrak{A}\mathfrak{X}}(\xi) = \sum_{m,i,j,l=1,3} \langle A_{\xi=0}^{qs} | m^{N-1} \rangle b_{mj}(0,\xi) V_{ji}^{ee} b_{il}(\xi,\tau_T)$$
$$\times \langle l^{N-1} | X_{\xi=\tau_T}^{qs} \rangle, \quad (63)$$

$$V_{\mathfrak{B}\mathfrak{X}}(\xi) = \sum_{m,i,j,l=1,3} \langle B_{\xi=0}^{qs} | m^{N-1} \rangle b_{mj}(0,\xi) V_{ji}^{ee} b_{il}(\xi,\tau_T)$$
$$\times \langle l^{N-1} | X_{\xi=\tau_T}^{qs} \rangle. \quad (64)$$
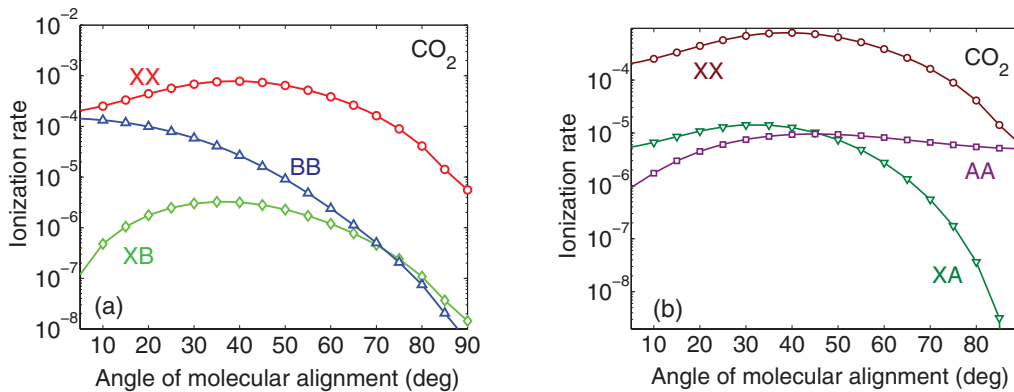
FIG. 5. (Color online) Angular-dependent ionization rates for direct XX (red circles), AA (violet squares), BB (blue triangles), and correlation-driven channels XB (a) (green diamonds) and XA (b) (green inverted triangles) in CO_2. Laser parameters are in the regime of nonadiabatic tunneling ($\gamma \geqslant 1$): $\lambda = 800$ nm, $I = 0.8 \times 10^{14}$ W/cm^2 laser field.
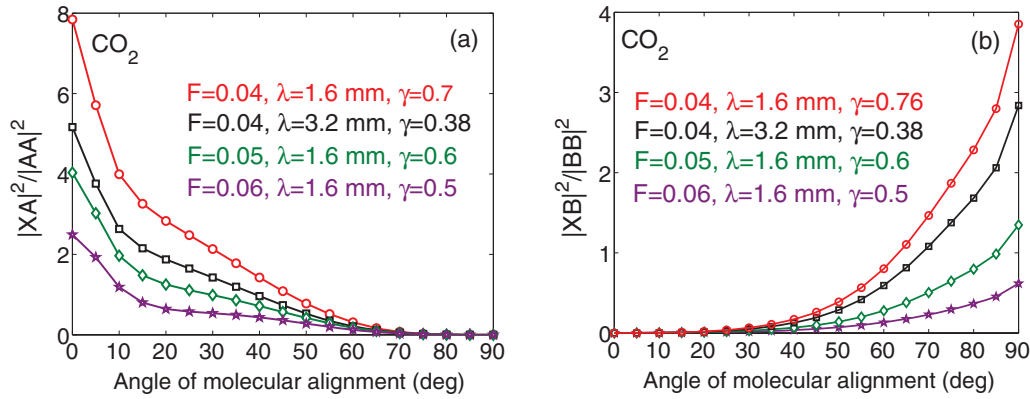
FIG. 6. (Color online) The ratio of ionization rates for correlation-driven and corresponding direct channels leading to the production of CO_2^+ in excited states A (a) and B (b) for different laser parameters in tunneling regime ($\gamma < 1$). (a) $F = 0.04$ a.u., $\lambda = 1.6$ μm (red circles); $F = 0.04$ a.u., $\lambda = 3.2$ μm (black squares); $F = 0.05$ a.u., $\lambda = 1.6$ μm (green diamonds); $F = 0.06$ a.u., $\lambda = 1.6$ μm (violet stars). (b) $F = 0.04$ a.u., $\lambda = 1.6$ μm (red circles); $F = 0.04$ a.u., $\lambda = 3.2$ μm (black squares); $F = 0.05$ a.u., $\lambda = 1.6$ μm (green diamonds); $F = 0.06$ a.u., $\lambda = 1.6$ μm (violet stars).

Detailed analysis of the properties of these potentials can be found in [40]. The excitation amplitude is given by their time integrals.

As seen in Fig. 2, correlation-driven channels play a very important role in the strong-field ionization of N_2. Here the correlation-driven XA channel is comparable to the the direct AA channel, while XB *always* dominates the direct BB channel. In this figure, we used laser parameters similar to experimental parameters in [24], which put the system in the regime of nonadiabatic tunneling ($\gamma \gtrsim 1$). As seen in Figs. 3 and 4, respectively, correlation-driven channels play a significant role in tunneling ($\gamma < 1$) and multiphoton regimes ($\gamma \sim 3$) as well.

In CO_2, shown in Figs. 5 and 6, the XB channel is significant for large but not for small alignment angles. The suppression at small alignment angles is due to the dipole coupling between the X and B states of the ion, which is maximized when the molecule is aligned perpendicular to the laser field and is zero for parallel alignment. For the same reason, the XA channel dominates at small angles, but drops at large angles. As seen in Fig. 6, a similar angular dependence applies in the tunneling regime. Note that the contribution of the direct BB channel shown in Fig. 5(a) is enhanced due to the Stark shift.

VII. CONCLUSIONS

Strong-field ionization is an intrinsically multielectron process. In contrast to the usual SAE approximation, the state of the electrons which do not escape the ion may evolve due to interactions with the departing electron, causing excitation of the ion and leading to attosecond dynamics of core rearrangement. These dynamics determine the initial conditions and the coherence of the hole created upon ionization. Novel ultrafast imaging techniques may allow one to time resolve core rearrangements upon strong-field ionization [21,24] and characterize the coherence of hole motion [25]. Thus, understanding multielectron excitations during strong-field ionization is crucial for controlling and imaging hole dynamics and its coherence [44] in atoms [25] and molecules. It is also important for applications such as

mass spectrometry with femtosecond infrared pulses. Here fragmentation patterns will strongly depend on the excitations of the molecular ions during ionization.

To describe these multielectron dynamics, we have developed a multichannel theory of strong-field ionization. In this theory, interaction with the departing electron couples different ionization channels and leads to new ionization pathways, which may compete with or even dominate the direct channels for ionization to a particular final state. We obtained simple analytical expressions for the ionization amplitudes for these channels using a saddle-point method in the spirit of PPT theory, well known for accurately describing strong-field ionization in single-electron systems.

Using this theory, we find that nonadiabatic excitations of the core are important under typical experimental conditions. Compared with direct tunneling from more deeply bound orbitals, the correlation-driven channel does not suffer the full exponential suppression accompanying the thicker tunneling barrier. This effect appears to be particularly strong for large values of the Keldysh parameter γ and large ΔI_p. When important, correlation-driven channels approximately follow the angular dependence of their parent direct channels.

We are now in a position to address the questions asked in the Introduction. Because the exponential suppression accompanying an excited ionic state is minimized if the excitation occurs just before the tunneling exit, diagrams where N_1 (the number of photons absorbed before electron-electron correlation) approaches $N_0 = I_p/\omega$ (the total number of photons required for ionization) will be favored over those with small N_1. Note that the derived analytical expressions incorporate all such pathways. This insight also sheds light on the question of higher-order contributions of the electron-electron correlation. Here, powers of the correlation which contribute to the direct amplitude by returning the core to its original state describe polarization of the ionic core induced by the outgoing electron. After accounting for the effects of this polarization, correlation-induced change of the ionic state is dominated by first-order terms, as higher-order diagrams are likely to involve the electron spending more time under a thicker tunneling barrier, with the accompanying exponential suppression.

Note added in proof. We would like to draw the reader's attention to a recent paper by M. Amusia [45]. It points out that the exchange between an electron tunneling from a deeply bound orbital and an electron in the HOMO, mediated by the electron-electron interaction, can enhance the amplitude of the deeply bound electron orbital in the classically forbidden region, leading to slower exponential decay in the classically forbidden region, consistent with the behaviour of the HOMO. The enhancement is proportional to the matrix element of the electron-electron interaction between the two electrons, and is mathematically similar to the enhancement discussed in this paper. We note, however, the fundamentally dynamic nature of effect discussed in our paper. We also bring the reader's attention to [46], where a similar effect and its role in double ionization has been analyzed classically and termed "precollision" [47].

[1] J. A. Tanis *et al.*, Phys. Rev. Lett. **83**, 1131 (1999).
[2] T. Schneider, P. L. Chocian, and J.-M. Rost, Phys. Rev. Lett. **89**, 073002 (2002).
[3] T. Schneider and J.-M. Rost, Phys. Rev. A **67**, 062704 (2003).
[4] L. Torlina and O. Smirnova, preceding paper, Phys. Rev. A **86**, 043408 (2012).
[5] L. V. Keldysh, Sov. Phys. JETP **20**, 1307 (1965).
[6] A. M. Perelomov, V. S. Popov, and M. V. Terentiev, Zh. Eksp. Teor. Fiz. **50**, 1393 (1966) [Sov. Phys. JETP **23**, 924 (1966)].
[7] S. V. Popruzhenko, V. D. Mur, V. S. Popov, and D. Bauer, Phys. Rev. Lett. **101**, 193003 (2008).
[8] B. A. Zon, Sov. Phys. JETP **91**, 899 (2000).
[9] A. S. Kornev, E. B. Tulenko, and B. A. Zon, Phys. Rev. A **68**, 043414 (2003).
[10] A. S. Kornev, E. B. Tulenko, and B. A. Zon, Phys. Rev. A **69**, 065401 (2004).
[11] A. S. Kornev, E. B. Tulenko, and B. A. Zon, Phys. Rev. A **79**, 063405 (2009).
[12] I. V. Litvinyuk, F. Legare, P. W. Dooley, D. M. Villeneuve, P. B. Corkum, J. Zanghellini, A. Pegarkov, C. Fabian, and T. Brabec, Phys. Rev. Lett. **94**, 033003 (2005).
[13] N. Pfeiffer Adrian, Claudio Cirelli, Mathias Smolarski, Darko Dimitrovski, Mahmoud Abu-samha, Lars Bojer Madsen, and Ursula Keller, Nat. Phys. **8**, 76 (2012).
[14] V. N. Ostrovskii, Zh. Eksp. Teor. Fiz. **84**, 1323 (1983) [Sov. Phys. JETP **57**, 766 (1983)].
[15] M. Ya. Ovchinnikova and D. V. Shalashilin, Khim. Fiz. **7**, 175 (1988).
[16] A. N. Pfeiffer, C. Cirelli, M. Smolarski, R. Dörner, and U. Keller, Nat. Phys. **7**, 428 (2011).
[17] A. N. Pfeiffer, C. Cirelli, M. Smolarski, Xu Wang, J. H. Eberly, R. Dörner, and U. Keller, New J. Phys. **13**, 093008 (2011).
[18] H. Rottke, J. Ludwig, and W. Sandner, J. Phys. B **29**, 1479 (1996).
[19] A. E. Boguslavskiy, J. Mikosch, A. Gijsbertsen, M. Spanner, S. Patchkovskii, N. Gador, M. J. J. Vrakking, and A. Stolow, Science **335**(6074), 1336 (2012).
[20] L. Young, D. A. Arms, E. M. Dufresne, R. W. Dunford, D. L. Ederer, C. Hohr, E. P. Kanter, B. Krassig, E. C. Landahl, E. R. Peterson, J. Rudati, R. Santra, and S. H. Southworth, Phys. Rev. Lett. **97**, 083601 (2006).
[21] O. Smirnova, Y. Mairesse, S. Patchkovskii, N. Dudovich, D. Villeneuve, P. Corkum, and M. Yu. Ivanov, Nature (London) **460**, 972 (2009).

[22] H. Akagi, T. Otobe, A. Staudte, A. Shiner, E. Turner, R. Dorner, D. Villeneuve, and P. Corkum, Science **325**, 1364 (2009).
[23] S. Haessler, J. Caillat, W. Boutu, C. Giovanetti-Teixeira, T. Ruchon, T. Auguste, Z. Diveki, P. Breger, A. Maquet, and B. Carre, Nat. Phys. **6**, 200 (2010).
[24] Y. Mairesse, J. Higuet, N. Dudovich, D. Shafir, B. Fabre, E. Mevel, E. Constant, S. Patchkovskii, Z. Walters, M. Y. Ivanov, and O. Smirnova, Phys. Rev. Lett. **104**, 213601 (2010).
[25] E. Goulielmakis *et al.*, Nature (London) **466**, 739 (2010).
[26] C. Wu, H. Zhang, H. Yang, Q. Gong, D. Song, and H. Su, Phys. Rev. A **83**, 033410 (2011).
[27] M. Spanner and S. Patchkovskii, Phys. Rev. A **80**, 063411 (2009).
[28] S. Petretti, Y. V. Vanne, A. Saenz, A. Castro, and P. Decleva, Phys. Rev. Lett. **104**, 223001 (2010).
[29] S. Patchkovskii, O. Smirnova, and M. Spanner, J. Phys. B **45**, 131002 (2012).
[30] O. Smirnova, M. Spanner, and M. Ivanov, Phys. Rev. A **77**, 033407 (2008).
[31] S. V. Popruzhenko and D Bauer, J. Mod. Opt. **55**, 2573 (2008).
[32] O. Smirnova, M. Spanner, and M. Ivanov, J. Phys. B **39**, S307 (2006).
[33] O. Smirnova, M. Spanner, and M. Yu. Ivanov, J. Phys. B **39**, S323 (2006).
[34] Olga Smirnova *et al.*, J. Phys. B **40**, F197 (2007).
[35] Misha Ivanov and Olga Smirnova, Phys. Rev. Lett. **107**, 213605 (2011).
[36] A. Friedman William, Ann. Phys. **45**, 265 (1967).
[37] C. Figueira de Morisson Faria and X. Liu, J. Mod. Opt. **58**, 1076 (2011).
[38] R. Murray, M. Spanner, S. Patchkovskii, and M. Yu. Ivanov, Phys. Rev. Lett. **106**, 173001 (2011).
[39] We use $|m^{N-1}\rangle$, $|n^{N-1}\rangle$ to represent field-free sates of the ion and $|\mathfrak{n}_{t''}^{N-1}\rangle$, $|\mathfrak{m}_{t''}^{N-1}\rangle$, for quasistatic states of the ion.
[40] Z. Walters and O. Smirnova, J. Phys. B **43**, 161002 (2010).
[41] R. Murray, W. K. Liu, and M. Y. Ivanov, Phys. Rev. A **81**, 023413 (2010).
[42] Z. X. Zhao, X. M. Tong, and C. D. Lin, Phys. Rev. A **67**, 43404 (2003).
[43] M. Abu-samha and L. B. Madsen, Phys. Rev. A **80**, 023401 (2009).
[44] N. Rohringer and R. Santra, Phys. Rev. A **79**, 053402 (2009).
[45] M. Ya. Amusia, JETP Lett. **90**, 161 (2009).
[46] Xu. Wang and J. H. Eberly, arXiv:1102.0221 [physics.atom-ph].
[47] J. Eberly (private communication).